A Novel Non-Contact Inspection Method for Measuring the Centering Error of Spherical Singlet Lens

Ping Sun *

The Institute of Optics, University of Rochester, Rochester, United States

* Corresponding author: psun9@u.rochester.edu

Abstract. As one of the important factors which can seriously affect the image quality, the centering error can be introduced during lens manufacturing and assembling process. Thus, the method to measure the centering error becomes a popular topic in industry. This study mainly introduces one new non-contact measurement method for spherical singlet lens's centering error. It includes two parts: test lens aligns with rotation axis by using powermeter to measure the unrefracted light power, and centering error is calculated by measuring the center trough position change in the diffraction pattern while rotating the test lens. According to the analysis, with specific optical layout design (fiber laser, collimated lens, aperture, three independent jaws precise rotary stage with test lens, powermeter / CCD with telecentric lens). Based on the results of multi-trials, it determines the alignment of the test lens on the rotary stage and finds the centering error of test lens χ=5.5798×10^{-4} arc. The precision of the result is also discussed. This method has advantages including economics, less complex operation procedure, high precision and sensitivity, large compatibility for all symmetric spherical lens, which provides another new and effective solution to measure the centering error in the lens manufacture and metrology industry.

Keywords: Centering error, lens alignment, diffraction, center trough position change.

1. Introduction

In the optical component industry, the decentration of optical component is one of the most important factors that people care about. While crafting, polishing, and assembling lenses, centering errors primarily arise from the wedging and decentering of the lens itself or from imprecise lens placement within the housing [1]. In detail, there are five kinds of centering errors specifically: (1) translational displacement of a lens; (2) tilt of a lens; (3) surface tilt error of a spherical surface; (4) cementing error and (5) tilt of the aspherical axis [2]. All of these errors are shown in Fig. 1.

These errors can seriously influence the imaging quality, detection efficiency of entire optical system. For instance, the decentration of lens can seriously imaging performance of mobile photon camera and introduce aberrations [3]. In that case, measuring and inspecting the decentration of optical component such as lens is very essential and becomes a hot topic. In fact, it is quite hard to test the centering of lens since some of errors are too small to be observed visually, but its effect is accumulated. In that case, the optical inspection is needed. In 1996, contact stylus instrument has been invented and used in the testament of rotationally symmetric aspheric surfaces [4].

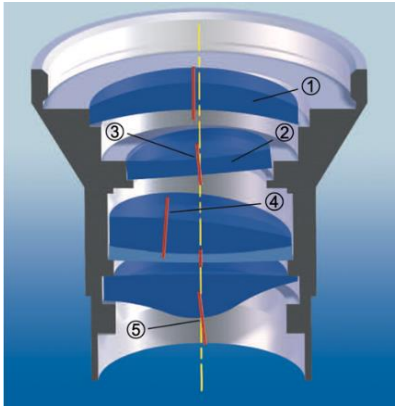

Figure 1. Five types of centering error.

Based on the mechanical method, the centering error can be measured but with low resolution and efficiency. Additionally, the sample region using this method is limited. Then, the earliest interferometric transducers are used which increases the measurement resolution [5]. Comparing with traditional contact method, nowadays, there are more advanced non-contact decentration inspection technique invented: analyzing the isogyres to yield the optical centroids [6], using Fizeau interferometer to analyze the interferogram of optical surface (seen from Fig. 2) [7], using the auto stigmatic microscope with precise rotary table to locate the centers of curvature of both surfaces [8].

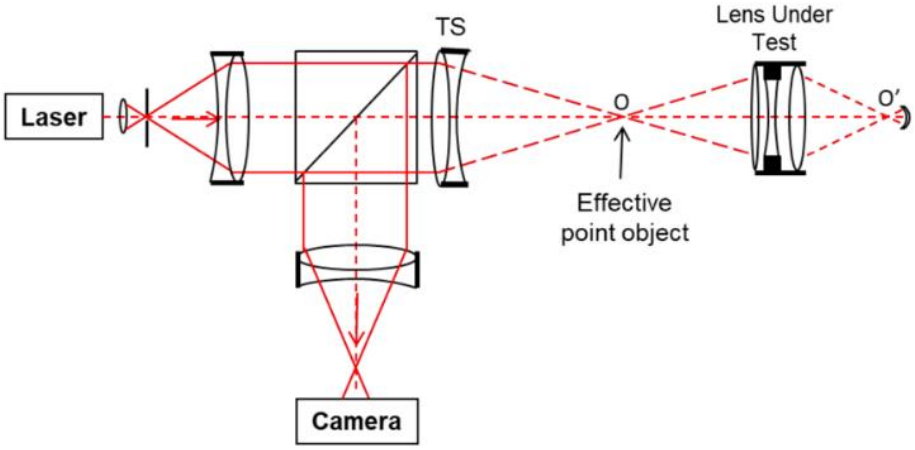

Figure 2. Fizeau interferometer layout .TS is transmission sphere and the o' is the center of curvature of the reflected mirror

One specific example is Optical Centering Machine from OptiCentric®. It mainly has two modes: reflection and transmission mode. For the reflection mode, while the test lens is placed and aligned with one ultra-precision rotary holder, one autocollimator with cross emits the light and focus on the center of curvature of the test surface. Ideally, since the light is perpendicular to the surface, the light will reflect and the image and object of cross should coincidence. However, when there is decentration, the reflection will change when rotating the lens which makes the image of cross moves on one circle. The radius of the trace out circle is proportional to the centering error of this test surface [2, 9]. For the transmission mode, especially same except now the light is focus on the focal plane of the test lens and analyze the image of cross to get the centering error for this lens ('overall error' of two surfaces) [2]. Both of modes yield very precise result. Nevertheless, there are certain shortcomings. The reflection mode does not work for the surface with antireflection coating. The alignment process is based on the mechanical with certain precise detector (or based on the special edge contact mounting [10]). The whole system is very expensive (~$1million). In addition, for other methods, there are still some limitations. For instance, the interferometer method requires complex testing procedure which lowers the testing efficiency. Thus, to lower the cost of centering error measurement and improve the existing inspection method, this paper investigates one new non-contact method to inspect the decentered spherical singlet lens, based on the transmission mode from OptiCentric®. This new technique uses three jaws chucks (each jaw can move independently) fixed on one precise rotary platform to hold the test lens. It uses power meter to align the lens on the precise rotary platform instead of using mechanical detector, lowering the requirement of mechanical structure but with high result precision. And this alignment system can be used for all spherical singlet lens with diameter from 16mm to 36mm and thickness up to 5mm. In addition, it uses the principle of diffraction rather than cross image which lose the requirement of focusing. In that case, this method's optical system is simpler and more economics which provide other decentration test choice for optical manufacturers. This paper will introduce the basic principle of centering error, diffraction, and Fourier transformation first. Then, it will turn to the designed optical layout in the lab and the detail experiment procedure with the experiment result. In final, the advantage and further investigation of this novel method will also be discussed.

2. Methodology

2.1. Centering Error

One optical lens has two important axes, i.e., geometry axis and optical axis. Geometry axis of the lens is just the axis of rotational symmetry which is defined by the circular edge of lens. The optical axis is relative to the center of curvature of the surfaces and for one incoming ray which is parallel to the optical axis of the optical lens, it will focus on the focal point of this lens [2, 11]. For the symmetric spherical singlet lens, only when these two axes coincidence, the lens is centered [2]. In that case, the basic principle to test the centration of the lens is to locate these two axes by using one another reference axis which is the rotation axis of the precise stage, shown in the left panel of Fig. 3. So, the first thing is to make the geometry axis coincidence with the rotation axis of the precise stage. This can be done by using the power meter with three independent jaws precise rotary platform. Once the geometry axis coincidence with the rotation axis of the precise stage, it can use the optical method to locate the optical axis and test whether the optical axis also coincidence with the rotation axis of the precise stage. If there is one certain deviation between these axes, it means that the test lens is decentered and have certain centering error. The centering error can be either expressed by an angle between the optical axis of the test lens and the reference axis (geometry axis or rotation axis of the precise stage) χ or the deviation distance between the center of curvature of the surface and the reference axis a. The definition of centering error is shown in right panel of Fig. 3. Based on the geometry, these two variables can be converted by:

$$\chi = \arcsin(a/r) \tag{1}$$

Where r is the radius of curvature of the surface [2]. About the method to locate the optical axis, traditional, one collimated light is used as similarly in transmission mode of OptiCentric® [2]. The basic structure and result are shown in Fig. 4 [9, 11].

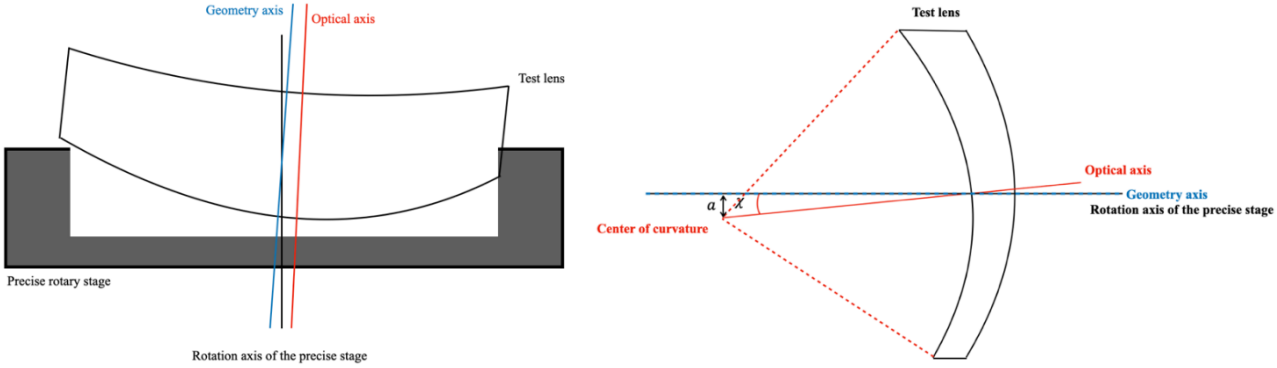

Figure 3. The plot of geometry axis, optical axis and rotation axis of the precise stage (left panel) and the definition of centering error in χ and a after the coincidences (right panel).

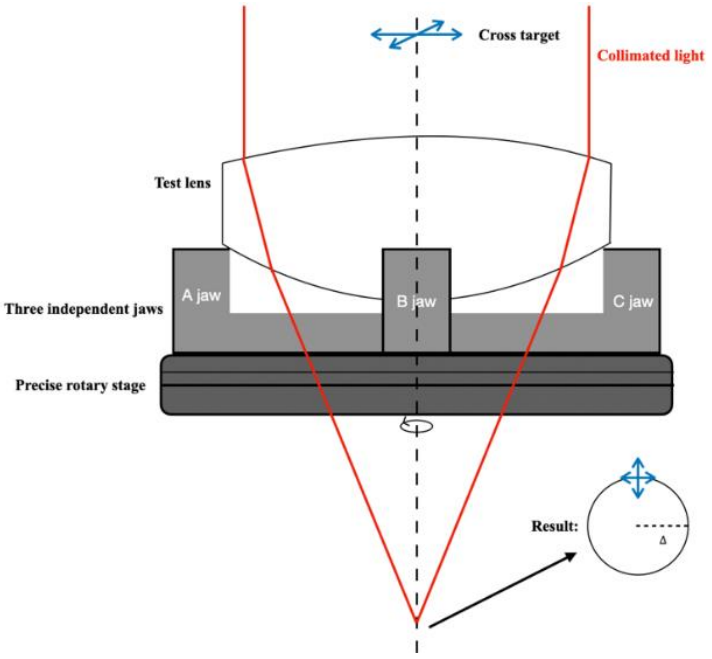

Figure 4. Traditional method to locate the optical axis.

Ideally, when there is no centering error, the image of cross target after refracting through the rotating lens with stage will not trace out a circle and the position of its image will not change. However, for the decentered lens, while rotating, the refracted light will change periodically, and the image will have a circle with radius Δ or ellipse trace. Based on the ray tracing, the radius of the trace-out circle is proportional to the centering error [9], and the centering error in this layout can be found by:

$$\delta = \frac{\Delta}{f}, \chi = \frac{\delta}{(n-1)} \tag{2}$$

Where f is the focal length of test lens, Δ is the trace-out image circle radius, n is the refractive index of the test lens. However, there is one shortcoming. Since normally the centering error is quite small and the trace-out circle is much smaller (the image of cross slightly moves). It needs to use detector with high resolution and sensitivity. In addition, to have a clear image, for each test lens, the detector needs to move along the axis correspondingly to focus which is less efficient. To make the effect of entering error more obvious, this paper introduces new methods which bases on the diffraction pattern rather than the image of cross, which has high sensitivity and no need to adjust focus.

2.2. Diffraction and Fourier transformation

Diffraction occurs when the light acting as the electromagnetic wave is obstructed by certain boundary, such as pinhole, finite aperture. Depend on the wavelength, boundary size, boundary shape, light wave will interference with each other and produce the specific dark-bright pattern on the screen [12]. The dark-bright pattern is called diffraction pattern or fringes, which highly relative to the phase of each light wave. One famous diffraction experiment is double fringes experiment in 1800s [13]. In the centering error inspection method, it uses one nearly-circle small aperture with diameter 3mm.

In the source plane, it can use the circ function to describe the source:

$$circ\left(\sqrt{x_s^2 + y_s^2}|\Delta_s\right) = 1, \sqrt{x_s^2 + y_s^2} < \Delta_s, circ\left(\sqrt{x_s^2 + y_s^2}|\Delta_s\right) = 0, \sqrt{x_s^2 + y_s^2} > \Delta_s \tag{3}$$

In this conditional equation, x_s and y_s is the coordinate on the source plane and Δ_s is the aperture radius. It also has such relation based on triangle and cylindrical coordinates:

$$\rho_s = \sqrt{x_s^2 + y_s^2}, x_s = \rho_s cos\,(\phi),\ y_s = \rho_s sin\,(\phi) \tag{4}$$

Thus, the conditional equation Eq.2.1.3 actually means within the aperture radius, circ function is 1 and outside the aperture, circ function is 0 which corresponds to the real application: only inside the aperture the light can transmit and form the source. Then, one uses the Fourier transform for the source function to get the detection function, use Eq.2.1.5

$$U_d(x_p, y_p, L_z) = Cu_o \int_s circ\left(\sqrt{x_s^2 + y_s^2}|\Delta_s\right) e^{-i2\pi \frac{x_s x_p + y_s y_p}{\lambda L_z}} dx_s dy_s \tag{5}$$

Where C is the constant, x_p and y_p are the detection plane coordinate and L_z is the distance between the aperture and detection plane. Substituting Eq. (4) into Eq. (5) to the cylindrical coordinates and solve for the source plane integral:

$$U_d(\rho_p, \phi_p, L_z) = Cu_o 2\pi\Delta_s^2\, Jinc(\rho_p, \phi_p, L_z), Jinc(\rho_p, \phi_p, L_z) = \frac{J_1(2\pi\rho_p\Delta_s/\lambda L_z)}{2\pi\rho_p\Delta_s/\lambda L_z} \tag{6}$$

For the jinc function, the function zero occurs at $x = 3.83$. From Eq. (6), the separation between first circle fringe is found:

$$\rho_p^{(0)} = \frac{1.22\,\lambda L_z}{D} \tag{7}$$

In fact, Eq. (6) is the diffraction pattern function of the circular aperture which is also called airy disk [12]. The source and diffraction pattern plot are shown in Fig. 5.

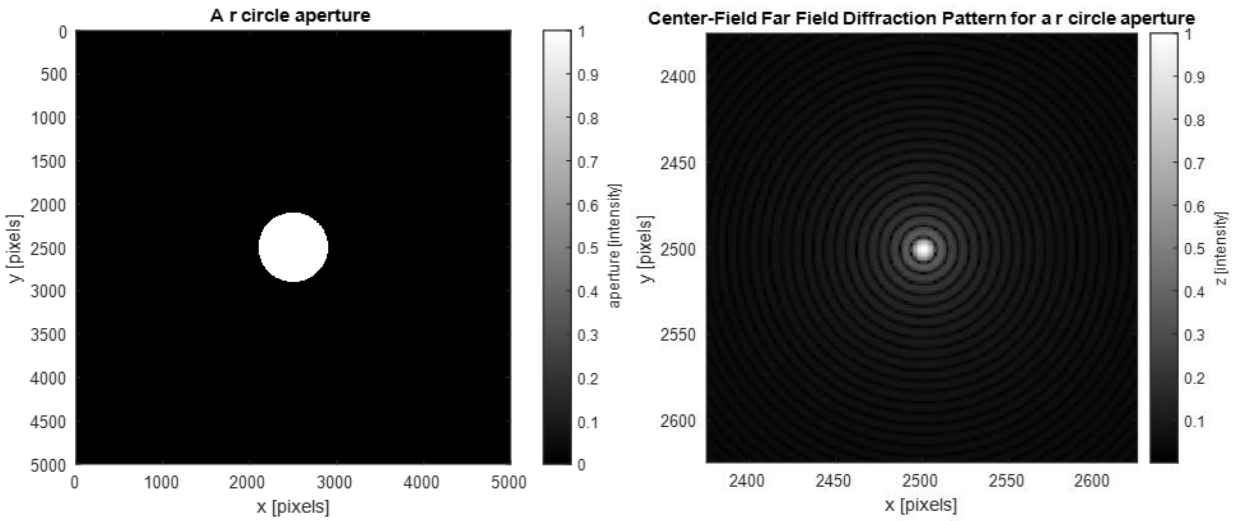

Figure 5. Source function (left) and diffraction pattern (right).

For the centering error measurement, it can be used to locate the optical axis of the lens without need to focus. The CCD is placed further back from the focus point which is very sensitive to any Airy disk center peak or trough position change due to decentered lens.

2.3. Optical Layout and Experiment Procedure

With the concept of centering error and diffraction, the following two optical layouts are used to inspect the decentration of lens as depicted in Fig. 6 and Fig. 7. For both configurations, it needs one collimated light. Thus, one 405nm Fiber Coupled Laser Module (FCM405S20UC1P1) is used which can produce clear TEM_00 mode with Gaussian profile. Because of its clear mode, it is no need to use laser mode filter. Then, one collimated lens with f=200mm is used to collimate the light. The

collimation is tested by precisely measuring the beam diameter after long distance. Then, the collimated light is obstructed by one AP with d=3mm. The diffraction occurs and the passed light will hit the test lens. The test lens is loaded on one special holder, which includes one three independent-adjusted jaws lens holder (CRD-V2X) and one precise rotary platform (GCM-1105M). The platform contains one hold in the middle enabling the refracted light to pass through. It can load and work for any singlet lens with diameter from 16mm to 36mm and thickness up to 5mm. In the experiment, the entire stage is fixed on the table (reduce vibration influence) and is rotated manually. One spherical singlet lens with diameter 24mm and focal length 100mm is tested in the experiment.

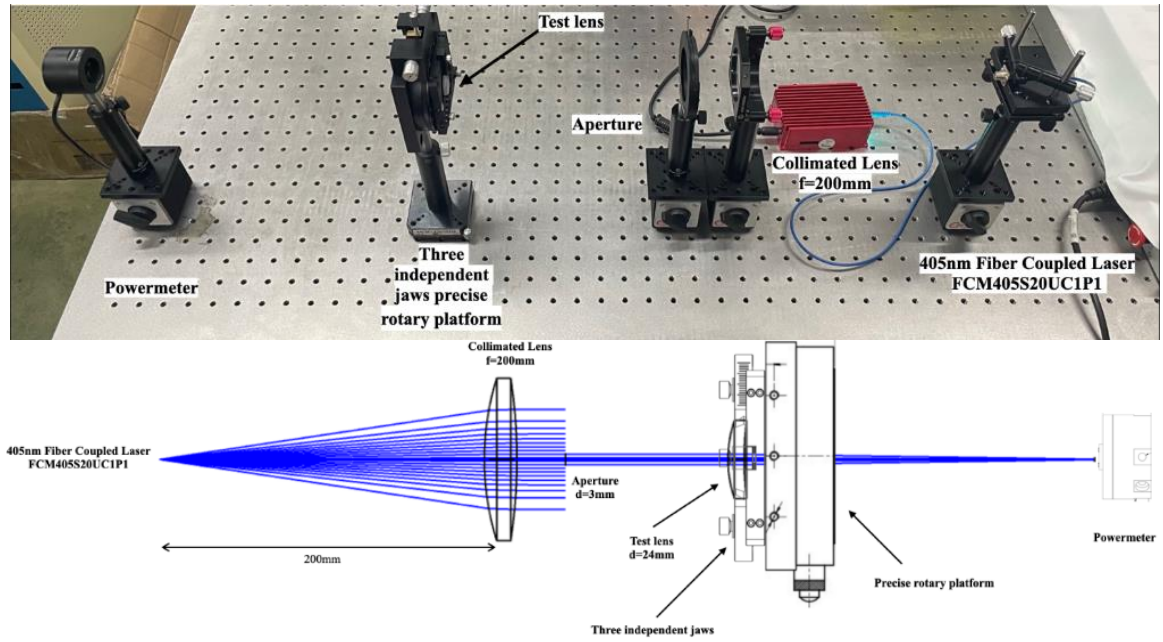

Figure 6. Optical layout for alignment test

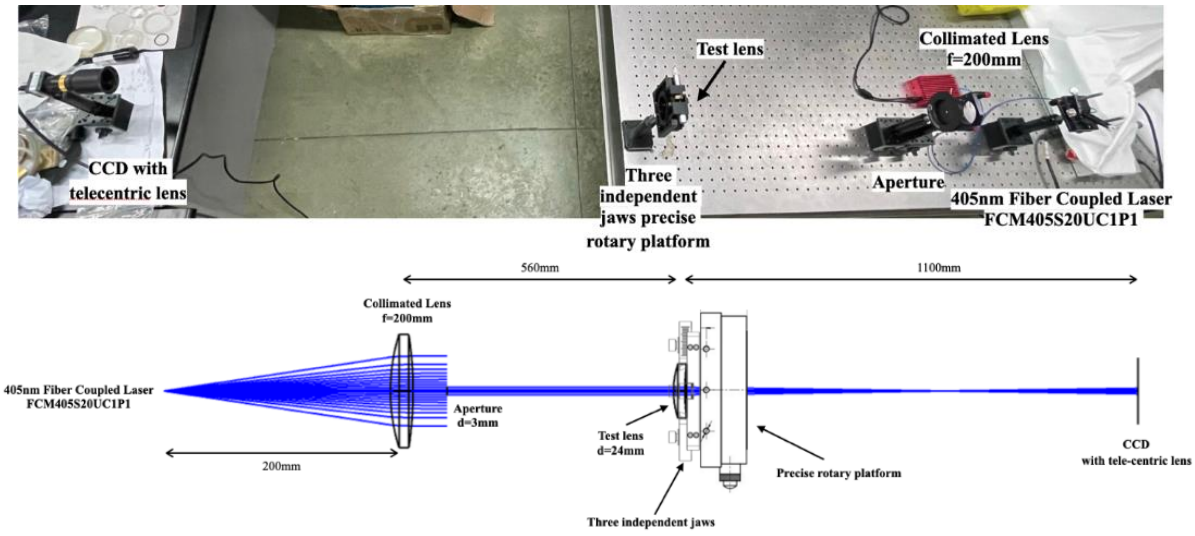

Figure 7. Optical layout for optical axis test

The experiment mainly divides into two parts, including alignment (Fig. 6) and test optical axis (Fig. 7). It mainly uses to coincidence the geometry axis with the rotation axis of the precise stage. Firstly, in the dark room, load the test lens on the holder roughly and place the holder with lens behand the AP, letting the light from AP to fully pass through the test lens. Adjusting the height and x y plane tilt of holder with test lens so that the reflected light from the test lens can return to the aperture hold (eliminate the lens's x y tilt). Translate the entire holder with test lens in the x axis on the table until ~50% light enter the lens and refract. The layout after translation is shown in Fig. 8. Now one part of

the light from aperture will enter the edge of test lens and refract to other direction, meanwhile another part of light will just pass through without entering the lens. These non-refracted light's power will be measured by the powermeter in the end. And since the refracted light deviates into different direction, it will not enter the power meter. Then, for well-aligned lens (the geometry axis of lens coincidences with the rotation axis of the precise stage), while rotating the test lens, the portion of non-refracted light should not have a periodic change. It means the reading on the power meter should not change periodically. Based on the power meter reading, the lens can be adjusted manually enabling the geometry axis of lens coincidences with the rotation axis of the precise stage. In the experiment, to better locate the problematic jaw, three jaws are named A B and C shown in FIG.2.2.2. And two power meter measurements are made on the left and right side of each jaw. In that case, there are six power meter readings, shown in Fig. 9. Through multi-trial measurement, each jaw position can be adjusted independently and precisely. It should be noted that at three jaws position, all light will be blocked thus power meter reading drops considerable. However, for other angle, this tech can provide specific and precise information about the alignment situation for the test lens.

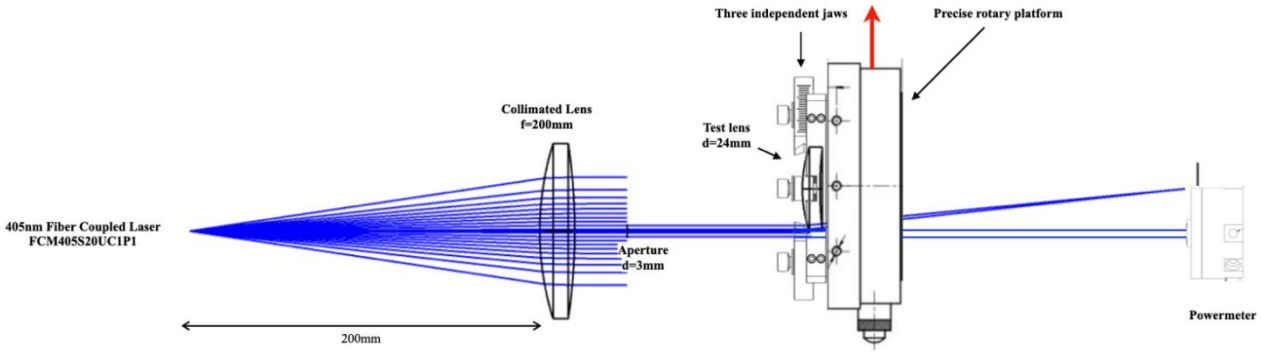

Figure 8. The translated layout.

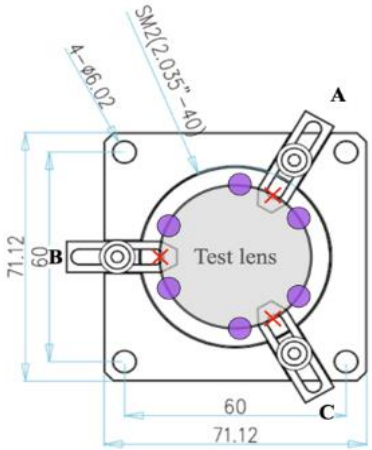

Figure 9. Six purple measured regions and three red crosses unmeasured regions.

Then, one uses layout in Fig. 7 to generate the diffraction pattern. As describe earlier, the diffraction pattern is relative to the aperture size and shape. The diffraction pattern will fully pass through and refract from the test lens. As the sensitive indices, diffraction pattern center trough position change can be used to analyze the centering error of the test lens while the lens is rotating. With the geometry axis of lens coincidences with the rotation axis of the precise stage, similarly, place the holder with test lens 560mm from the AP and place the CCD with tele-centric lens 1100mm from the test lens. At this time, allow all light from AP to pass through the test lens. In fact, it does not limit the full beam position on the test lens (unnecessary to pass the center of lens), because of its symmetry of test lens. Then one adjusts to eliminate the x y tilt of lens. Since whether the center of diffraction pattern is peak or trough depends on the optical path difference and phase difference, one needs to slightly move the CCD until getting one pattern with clear and darkest center trough and use

CCD to record the pattern while rotating the test lens. Then, by imaging analyze, the trace-out position change of center trough on the diffraction pattern can be found and used for centering error calculation. Notes that the ratio between image pixel and physical distance should be found first in order to convert the trace-out position change from pixel to physical distance. The method is that firstly remove the holder and test lens. Place the CCD with telecentric lens at 3.7m from the AP. The light from AP directly enters the CCD. Adjust the diameter of AP so that just before entering the CCD the image size is 1cm and record the image. Use ImageJ to measure the diameter of this image in pixel number and this image corresponds to 1cm image size. Thus, the ratio between pixel and physical distance can be found. With 918-pixel image diameter, the ratio of pixel and mm is $R = 0.0109\ mm/pixel$. One also needs to modify since the diffraction pattern center trough is used instead of image of cross target because of the similar triangle property as given in Fig. 10. One can find following which is used for diffraction center trough target centering error measurement system:

$$\delta = \frac{E/11}{f}, \chi = \frac{\delta}{(n-1)} \tag{8}$$

where E is the diffraction center trough trace-out position change E. Thus, use ratio between pixel and mm, Eq. (8), and E, the centering error can be found. Since it uses diffraction pattern as the indices, there is no need to focus. In addition, the diffraction pattern center trough position is very sensitive which can have high resolution of centering error.

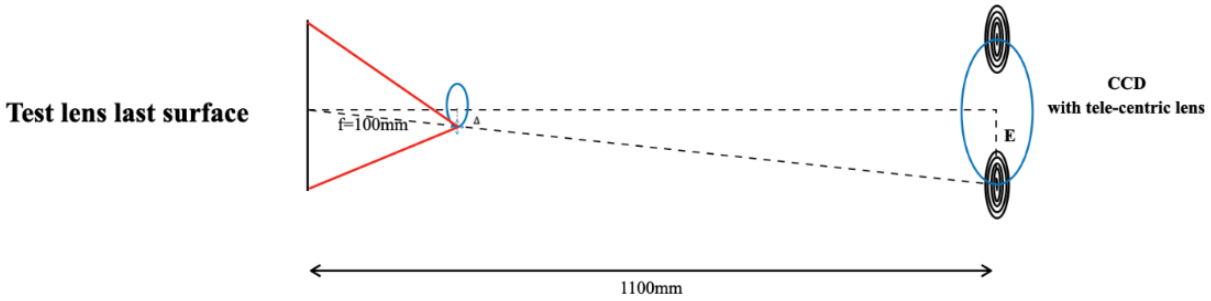

Figure 10. Similar triangle related to the trace-out cross circle radius Δ and diffraction center trough trace-out position change E.

3. Results and Discussion

The power meter result of initial rough loading is shown in Fig. 11. As described earlier, because in the initial rough loading, the geometry axis of lens does not coincidence with the rotation axis of the precise stage. Thus, when rotating the stages, the lens does not rotate circularly, and it will cause the measurement of power meter from unrefracted light (does not enter the lens) to be periodic as shown in Fig. 11. There existing great changes about 30uW. However, after the Part 1: alignment, 10 trials tests have processed and the result of 10 trials is shown in Fig. 12.

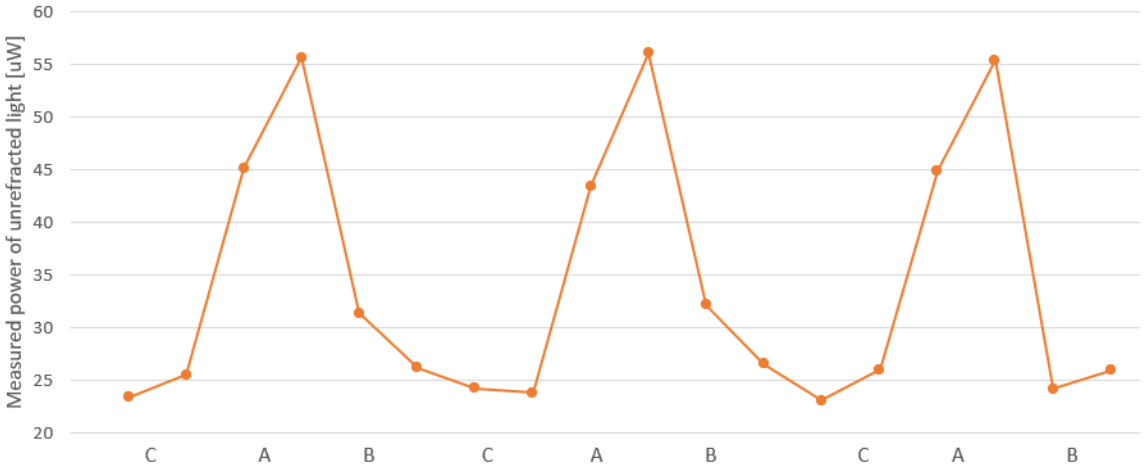

Figure 11. Continue 3 rotation cycles initial rough alignment power meter result.

Comparing with the Fig. 10 and Fig. 11, the alignment is much better (the geometry axis of lens coincidences with the rotation axis of the precise stage). And from FIG.3.2 data, it can find the standard deviation of 10 trials after Part 1: alignment is just about 0.3uW which is quite small. And the reason for such deviation is due to the detector dark current noise, the unsmooth edge of test lens, and the background vibration, which is so small that can be ignored. And the mean value of unrefracted light power is $37.4uW$ out of total $82.3uW$, which means on average 45.4% light does not enter and refract on the lens. In that case, it can site that the geometry axis of test lens coincidences well with the rotation axis of the stage. To be convincing and precise, the experiment takes 38 rotation angles diffraction pattern image and use MATLAB code to fit (reduce the influence of noise). Then, find the minimum intensity (center trough). Since the center trough is the key, plots are limited within the center region. The recorded diffraction pattern at 0-degree test lens rotation and its cross-section array (blue line) plot is shown in Fig. 13.

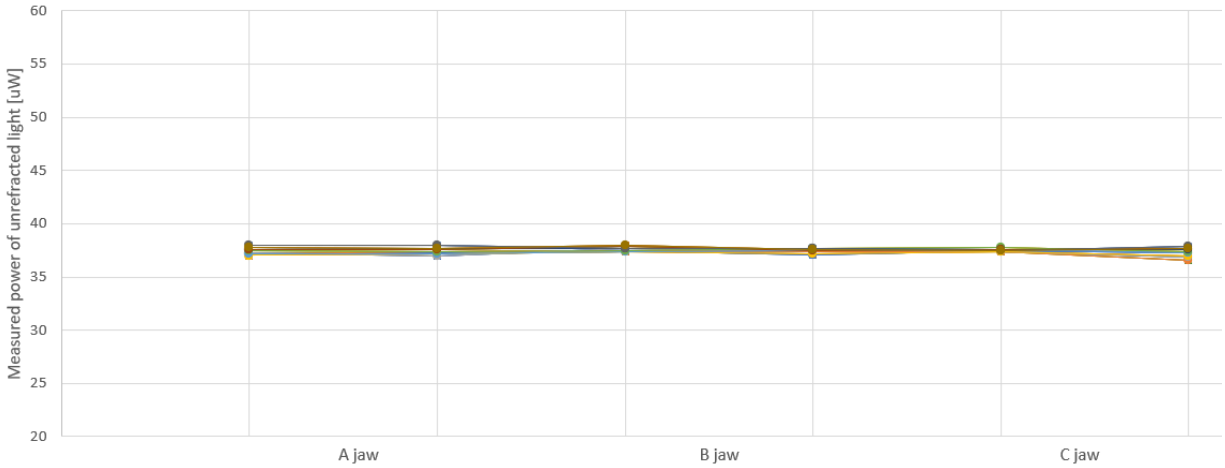

Figure 12. The power meter result over 10 trials after alignment.

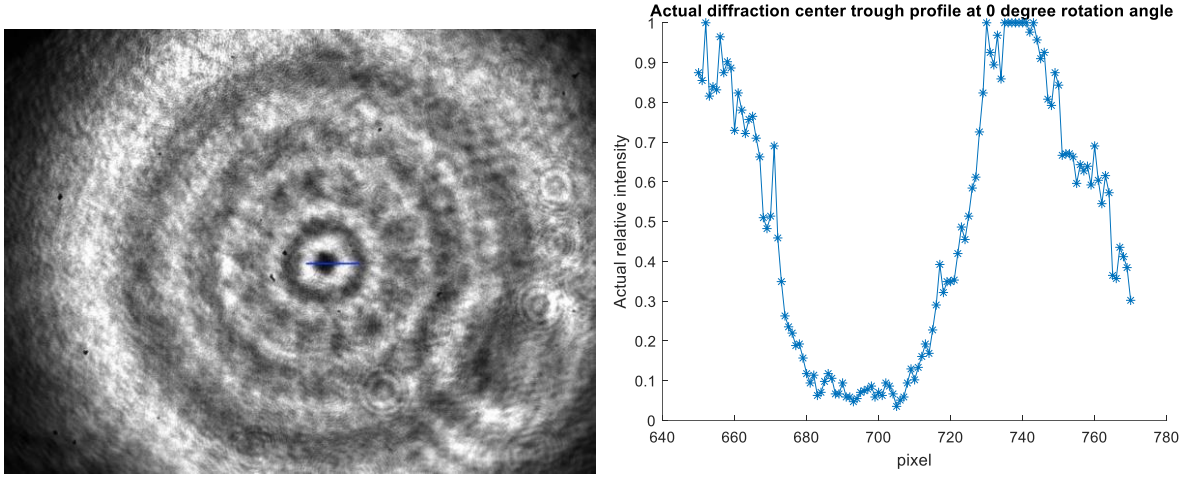

Figure 13. Diffraction pattern (left) and profile (right) at 0-degree test lens rotation.

Then, all 38 angles diffraction center trough fitted profile and trough location is shown in FIG.3.4

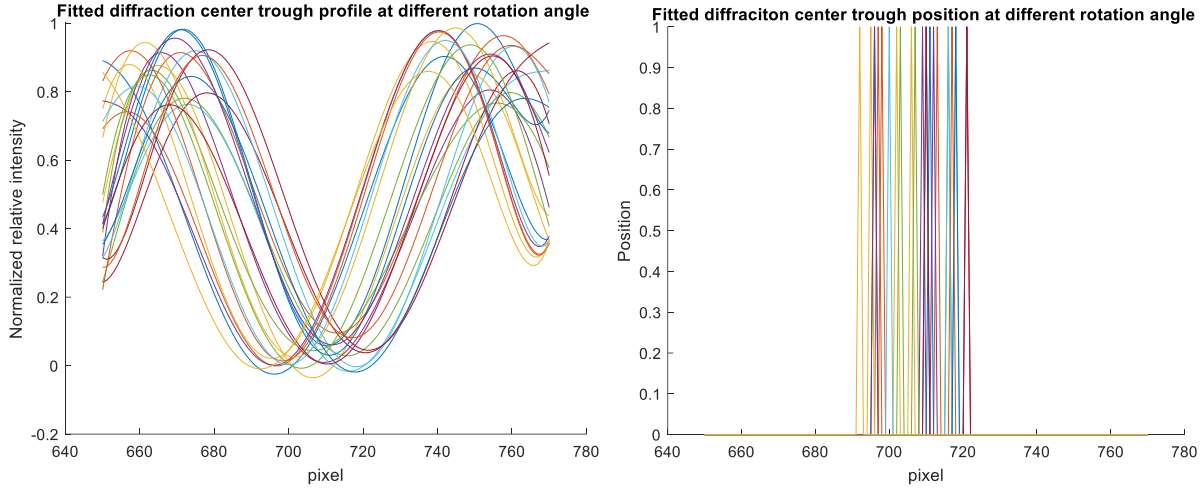

Figure 14. All 38 angles diffraction center trough fitted profile (left) and trough location (right)

From right panel of Fig. 14 right, it found the maximum (diameter) of center trough position change in pixel $E_p = 29\,pixel$. One can find the centering error angle $\chi = 5.5798 \times 10^{-04}\,arc$, which is quite small. Also, to test the influence of noise, such as vibration, detector noise, all 0-degree rotation results are compared within these 38 angles. Ideally, without any noise, when the rotation angle is 0, 360, 720… degree the center trough should return to the initial positions. As shown in Fig. 15 it can find that at 0 and 360 degree two profiles are almost same. Comparing with their trough position, their separation is just about 3 pixels. This means the system has much small noise and has high precision. Since this method bases on the diffraction pattern in the far field instead of cross image in the focal point, it will be more sensitive to any slight test lens surface change while rotating. Thus, after continuing reducing the noise and other vibration, this method's test resolution will be very high.

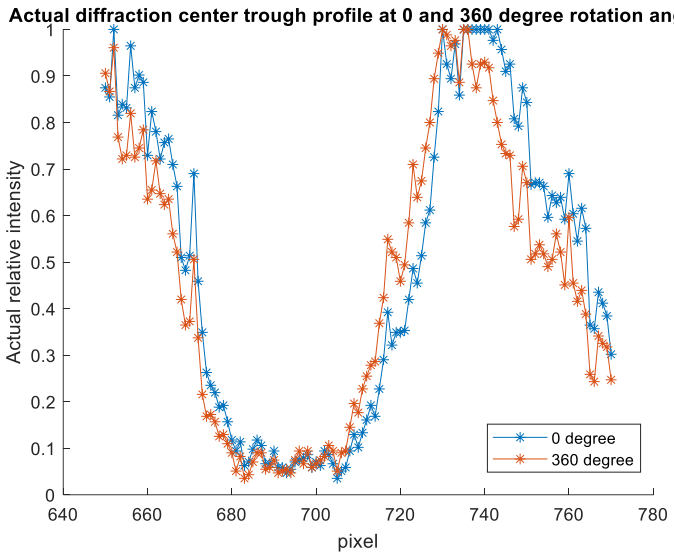

Figure 15. The center region diffraction profile at 0- and 360-degree rotation.

4. Limitaions and Prospects

This novel centering error method has certain limitation and need further investigation. For the shortcoming, until now it limits to test the spherical symmetric singlet lens and the result is about the 'overall' effect of two surfaces decentration and the precision can be higher. To solve the issues, firstly, it can work on other non-symmetric lens, such as aspherical lens, by using advance ray tracing to locate the ideal trace-out path of center trough on the diffraction pattern. The deviation of the actual path from the ideal represents the centering error on the test lens. Also, in fact, the traditional reflection mode and this novel method can use together. Reflection mode can calculate the error on one surface and it can subtract from the 'overall' effect based on the novel method to get the error on another surface. In addition, to increase the precision, some improvements to the optical layout can be used: e.g., the optical cage system to eliminate the x y plane tilt of each optical element. Besides, one can construct the precise slide to move the entire holder with test lens in the x direction [14]. Otherwise, one can use vertical system instead of horizontal on the table to eliminate the effect of gravity on the test lens. In fact, it is necessary to use more precise hold the lens, recommend using vacuum chuck which creates vacuum to cement the test lens in the position on the rotation stage [2]. Moreover, to reduce the vibration of stage rotation, one stable electrical machinery should be used to rotate the holder with the test lens instead of manually. Moreover, it is suggested to reduce other vibration source, one Air Bearing Table should be used.

5. Conlusion

To sum up, this paper mainly focuses on one new centering error measurement method for spherical singlet lens. After optical investigation and design, the method includes two parts. The first part is to align the lens and let the geometry axis of lens coincidence with the rotation axis of the stage by using power meter to measure the unrefracted light power change. The second part is to use center trough position change in the diffraction pattern to calculate the centering error. Besides, the centering error angle of the test lens is found $\chi = 5.5798 \times 10^{-04}\ arc$ with high precision. Although it has certain limitation, such as limit for symmetric surface, these shortcomings can be solved by further investigation and more precise equipment support. In that case, the total system has considerable potentials, including more economics, less complex operation procedure, high precision and sensitivity, large compatibility for all symmetric spherical lens. In fact, this method really becomes one alternative and effective solution for optical manufacturer in the lens metrology.

References

[1] Blanchard J. Elastomeric Mounting of Lens Elements. University of Arizona, OPT, 521: 4 - 5.

[2] Opti Centric ® . Opti Centric ® : Inspection, Alignment, Cementing and Assembly of Optics: Vol. 36.

[3] Chang C C, Wu Y, Lee C C. Error compensation in reflection type centering error testing. Optical Review, 2009, 16 (2): 149 - 152.

[4] International Standards Organization, Zurich. Geometrical Product Specifications (GPS) — Surface texture: Profile method: Nominal characteristics of contact (stylus) instruments[J]. International Standards Organisation, 1996, 13.

[5] Scott P J. Recent Developments in the Measurement of Aspheric Surfaces by Contact Stylus Instrumentation SPIE Digital Library, 2002.

[6] Chang C Y, Ma C C, Huang K C, et al. Rapid inspection method for measuring interior tilt and decenter in singlet lens. Applied Optics, 2013, 52 (4): B70.

[7] Dörband B, Seitz G. Interferometric testing of optical surfaces at its current limit. Optik, 2001, 112 (9): 392 - 398.

[8] Parks R E. Lens centering using the Point Source Microscope. Proceedings of SPIE, 2007.

[9] Heinisch J, Dumitrescu E, Krey S. Novel technique for measurement of centration errors of complex completely mounted multi-element objective lenses. SPIE Digital Library, 2006.

[10] Lamontagne F, Savard M, Desnoyers N, et al. High accuracy lens centering using edge contact mounting. Optical Engineering, 2021, 60 (05).

[11] Edmund OPTICS. Understanding Optical Specification. Edmund Optics. Retrieved from: https://www.edmundoptics.com/knowledge-center/application-notes/optics/understanding-optical-specifications/.

[12] Vamivakas N. Introduction to Wave Optics. University of Rochester, 2022, 140.

[13] Double slit experiment. Retrieved from: https://www.discovery.com/science/Double-Slit-Experiment.

[14] OpticsCage+ Optical Cage System. Retrieved from: https://www.newport.com/c/optics-cage-plus.